

Effect of processing conditions on microstructure and mechanical behaviour of metals sintered from nanopowders

Jenő Gubicza^{1,a}, Guy Dirras^{2,b} and Salah Ramtani^{2,c}

¹Department of Materials Physics, Eötvös Loránd University, Pázmány Péter s. 1/A, H-1117 Budapest, Hungary

²Laboratoire des Sciences, des Procédés et des Matériaux, Université Paris 13, 99, avenue Jean Baptiste Clément, 93430 Villetaneuse, France

^agubicza@metal.elte.hu (corresponding author), ^bdirras@univ-paris13.fr, ^cramtani@univ-paris13.fr

Keywords: Nanopowder, Sintering, Microstructure, Strength, Ductility.

Abstract. The influence of the consolidation conditions on the microstructure and plastic behavior of ultrafine-grained Ni and Al sintered from nanopowders was studied. It was found that the smaller initial Ni powder particle size yielded a smaller grain size and a larger oxide content in the as-consolidated sample resulting in a higher strength and lower ductility. When the Ni nanopowder was in contact with air (instead of an inert atmosphere) during the short handling time before sintering, the oxide content increased without a considerable change of the grain size that also decreased the ductility. The reduced time and temperature in Spark Plasma Sintering compared to Hot Isostatic Pressing led to a smaller grain size that resulted in a higher strength of Ni. In the case of an Al nanopowder processed by Hot Isostatic Pressing at 450 °C, the consolidation was hindered by the strongly limited diffusion due to the presence of a rigid amorphous layer on the surface of particles. However, at the sintering temperature of 550 °C, the crystallization and the fragmentation of the layer occurred that yielded a better densification.

Introduction

Nano- and ultrafine-grained (UFG) bulk metallic materials are usually processed by “bottom-up” or “top-down” methods [1]. The former group of methods includes the consolidation procedures of nanopowders while the latter processing routes are based on severe plastic deformation of conventional coarse-grained materials. Generally, nanopowder consolidation techniques result in texture-free microstructures that yield isotropic physical and mechanical behaviours of the sintered products. In most cases, contamination, formation of an oxide phase and remaining porosity are the by-products of consolidation techniques due to the large surface area of nanopowders [2]. These features have strong effects on the strength and ductility of sintered metals [3]. Previous studies showed that the microstructure (grain size, lattice defect densities, porosity, oxide phase content) of consolidated nanomaterials is strongly influenced by the conditions of sintering [4,5]. In this study, the effects of initial powder particle size, powder handling atmosphere, sintering method and temperature on the microstructure and mechanical behaviour of metals consolidated from nanopowders are investigated.

Experimentals

Ni nanopowder with the average particle size of 100 nm was produced by electro-explosion of Ni wires [6,7]. The powder was consolidated by Hot Isostatic Pressing (HIP) or Spark Plasma Sintering (SPS) method. Before HIP-processing, the powder was heat-treated in a capsule under hydrogen flow at 400°C and the capsule was sealed under inert gas (Ar) for preventing oxidation. During HIP method, the capsule was subjected to a pressure of 140 MPa at 700 °C for 150 min. In order to study the effect of sintering method, another sample was processed in Ar by SPS. During SPS procedure,

the powder was held under a pressure of 150 MPa at 500 °C for 1 min while pulses of high current density (of the order of 1000 A/cm²) were applied to the sample for promoting consolidation. The most important advantage of the latter method is that the compaction occurs more quickly and at much lower temperatures than in the case of HIP, thus preventing grain growth. The influence of the powder handling atmosphere during SPS on the microstructure was investigated by producing a specimen, for which the capsule containing the Ni nanopowder was broken in air instead of Ar and rapidly transferred to the mould. An additional sample was compacted by SPS from a Ni powder with the particle size of 50 nm in order to study the effect of initial particle size on the microstructure of SPS-processed materials. The phase composition of the Ni powders and the consolidated specimens were studied by X-ray diffraction using a Philips Xpert powder diffractometer with CuK α radiation. The grain size of the sintered samples was determined by transmission electron microscopy (TEM) using a JEOL-2011 electron microscope operating at 200 kV. The mechanical behavior was investigated by compression using an Instron universal testing machine (model 1195) at room temperature and an initial strain rate of 10⁻⁴ s⁻¹ up to the failure of the specimens. Additionally, the effect of HIP temperature on the microstructure of Al samples consolidated from a nanopowder was also studied. The powder particles with an average size of 80 nm were produced by electro-explosion of Al wires. The HIP was performed at 450 or 550 °C under a pressure of 200 MPa for 600 min. The phase composition and the microstructure were studied by X-ray diffraction and TEM, respectively.

Results and discussion

Comparison of microstructures and mechanical behaviours of Ni consolidated by HIP and SPS. The parameters of the microstructure of UFG Ni sintered from a nanopowder with an average particle size of 100 nm in Ar by HIP and SPS are compared in Table 1. In addition to the Ni phase, NiO was also detected by X-ray diffraction both in the powder and the consolidated specimens. Energy filtered TEM images have revealed that in the initial powder the most of oxide was found on the surface of nanoparticles [5]. For comparison of the NiO phase content in the different samples, the integrated intensity ratio of the X-ray peaks of NiO and Ni at 2 Θ =37.4° and 44.6°, respectively, is determined. It should be noted that this ratio does not give the NiO phase content in the samples, it is only proportional with the volume fraction of NiO phase. The intensity ratio for the initial powder was found to be 0.5 ± 0.1 % which does not change significantly during either HIP- or SPS-processing performed in Ar. TEM images presented in our previous publications [3,5] revealed that the average grain size in the consolidated samples is 3-4 times larger than the particle size in the initial powder, i.e. a grain-growth occurred due to the high temperature of sintering. The grain sizes in the samples processed by HIP or SPS are 403 or 306 nm, respectively. The reduced time and temperature of consolidation during SPS compared to HIP resulted in a lower grain-growth yielding a higher strength without altering the strain to failure during compression (see Table 1 and Fig. 1).

Table 1: The relative mass density, the intensity ratio ($I_{\text{NiO}}/I_{\text{Ni}}$) of the X-ray peaks for NiO and Ni at 2 Θ =37.4° and 44.6°, respectively, the mean grain size (d) determined from TEM images, the yield strength and the strain to failure obtained by compression for Ni samples processed from nanopowders by HIP or SPS.

Powder particle size [nm]	Consolidation conditions	Relative density [%]	$I_{\text{NiO}}/I_{\text{Ni}}$ [%]	d [nm]	Yield strength [MPa]	Strain to failure
100	HIP in Ar	95.5	0.5 ± 0.1	403	542	0.35
100	SPS in Ar	94.0	0.6 ± 0.1	306	660	0.33
100	SPS in air	95.4	0.9 ± 0.1	294	682	0.21
50	SPS in air	94.5	1.5 ± 0.1	250	1022	0.04

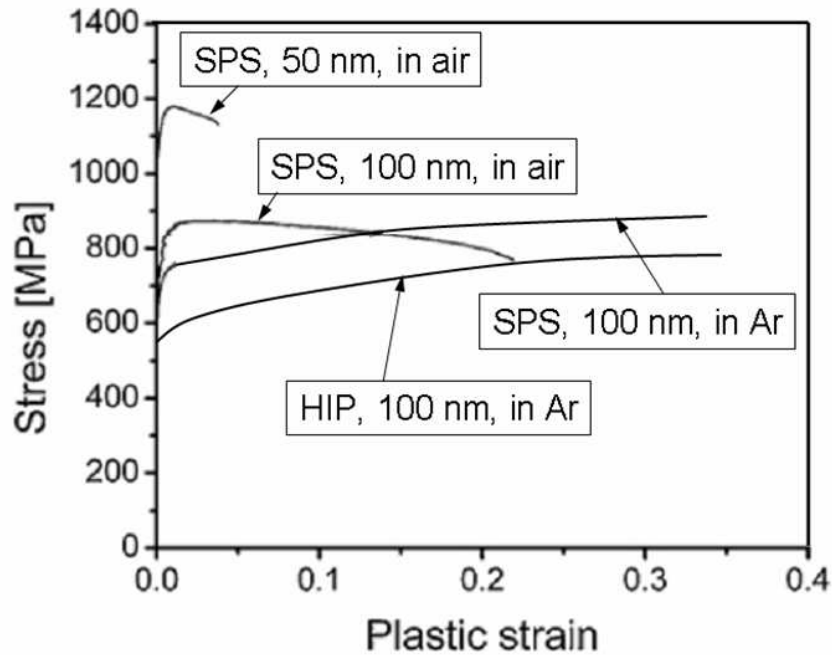


Fig. 1. Compression stress–strain curves for Ni samples consolidated by HIP or SPS from powders with the particle size of 50 or 100 nm. The powders were handled in Ar or air before sintering.

Effect of powder handling atmosphere and initial particle size on microstructure and mechanical properties of Ni. In order to study the effect of the powder handling atmosphere on the microstructure and plastic properties of Ni, an additional sample was processed by SPS for which the capsule containing the nanopowder with the particle size of 100 nm was broken in air instead of Ar. The processing in air yielded an increase of the NiO content from 0.5 ± 0.1 to 0.9 ± 0.1 % during sintering but did not have a significant influence on the grain size as it has been revealed in our recently published TEM study [3,5]. The grain size values are 306 and 294 nm for the specimens processed in Ar and air, respectively. Table 1 and Fig. 1 show that the higher oxide content in the latter sample resulted in a larger yield strength and a much smaller strain to failure. In addition, after an early saturation of the flow stress a work-softening was observed till the failure while the specimen processed in Ar exhibited work-hardening in the entire strain regime. The strain softening and the smaller ductility of the sample processed in air can be explained by the higher oxide content that resulted in a higher flow stress level during deformation, leading to a larger probability of debonding between grain boundaries. In addition, it is hypothesized that the higher total oxide content in this specimen probably involves larger oxide content on the grain boundaries, which may reduce the grain boundary strength, resulting in easier cracking during deformation.

For investigating the effect of the initial powder particle size on the microstructure and mechanical behavior of SPS-processed Ni, an additional sample was compacted from a Ni powder with the average particle size of 50 nm. This powder was handled in air before sintering. The microstructures of the specimens sintered from the powders with the average particle sizes of 100 and 50 nm are shown in Figs. 2a and b, respectively. The grain size of the latter sample was 250 nm that is only slightly smaller than the size of grains (294 nm) in the specimen processed from the powder with two times larger particle size. At the same time, the NiO content is much higher in the sample consolidated from the smaller particles (see Table 1) since the majority of NiO was most probably located on the surface of powder particles. Both Fig. 1 and Table 1 show that the specimen sintered from the powder with smaller particle size has higher strength but much lower ductility due to the smaller grain size and higher oxide content in the consolidated metal.

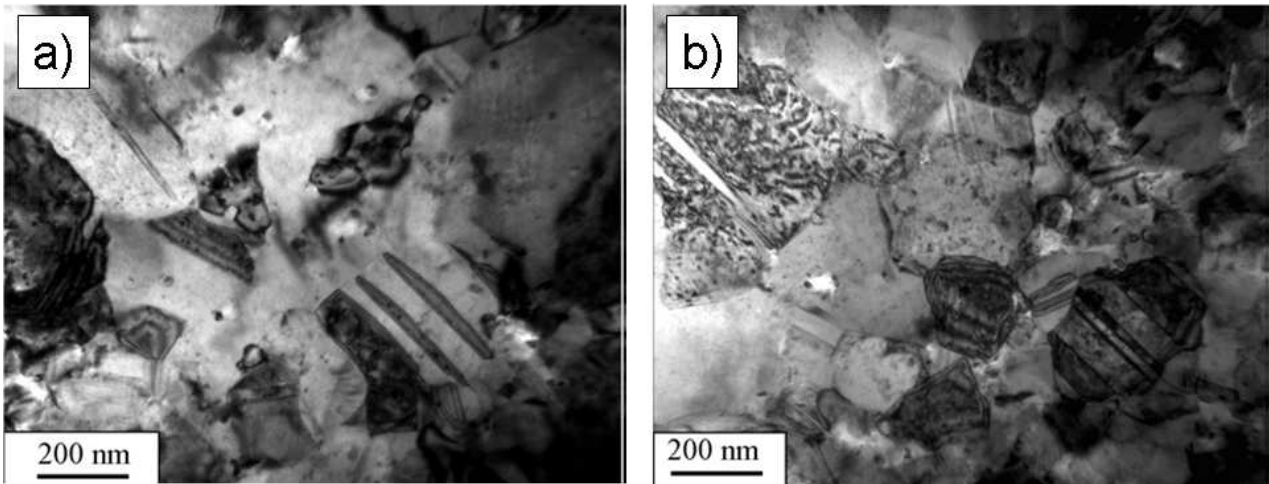


Fig. 2. TEM images of the microstructure of Ni samples consolidated by SPS from nanopowders with the particles sizes of (a) 100 nm and (b) 50 nm.

Influence of consolidation temperature on microstructure of Al processed from a nanopowder. The effect of sintering temperature on the consolidation of nanocrystalline Al powder was also investigated. The nanopowder consisted of particles with spherical shape and an average diameter of about 80 nm, however, a small amount of large particles with sizes between 1 and 60 μm was also observed [8]. In addition to Al, other crystalline phase was not detected in the powder by X-ray diffraction. At the same time, in the bulk material consolidated by HIP at 550 $^{\circ}\text{C}$, crystalline $\gamma\text{-Al}_2\text{O}_3$ was observed. Energy filtered TEM images revealed that the alumina phase existed in the form of dispersoids in the UFG Al matrix. As an example Fig. 3a shows the oxygen map of a thin foil where the dispersoids enriched in oxygen appear in white. These alumina dispersoids were most probably formed by crystallization of the native amorphous layer on the surface of powder particles as suggested by a previous work of Rufino et al. [9]. The crystallized alumina skeleton was broken due to the stresses developed during sintering thereby creating Al_2O_3 dispersoids in the consolidated material. The microstructure of the Al matrix consisted of UFG grains with an average grain size of about 150 nm and some embedded coarse grains with the size of 2-10 μm (see Fig. 3b). In addition to coarse particles already present within the initial powder, some of the observed coarse grains may have been grown during the HIP-processing but the fragmentation of the very large particles into smaller grains during sintering was also observed [10].

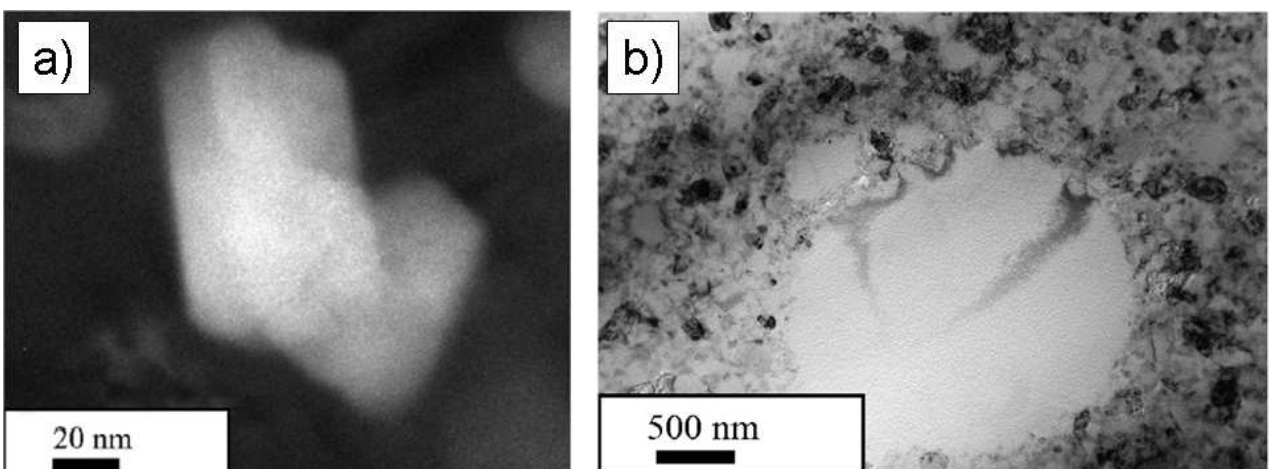


Fig. 3. (a) Energy filtered TEM image showing alumina dispersoids in Al consolidated at 550 $^{\circ}\text{C}$ by HIP. Oxygen-rich regions appear in white. (b) TEM picture of the Al matrix for the same sample.

In order to study the effect of HIP temperature on the microstructure, an additional sample was sintered at 450 °C. The sample consolidated at 450 °C exhibited a lower mass density than for the specimen HIP-processed at 550 °C as a consequence of incomplete sintering. This is supported by Fig. 4, where the TEM image taken on the sample processed at 450 °C shows undeformed spherical grain shape together with a significant porosity. X-ray diffraction revealed that crystalline alumina was not formed during sintering at 450 °C [11]. However, when this sample was heated up in a Differential Scanning Calorimeter, Al₂O₃ was crystallized at about 527 °C as indicated by former X-ray diffraction experiments [11]. Most probably, the surface of the initial powder particles were covered by a native amorphous layer [12] that transformed into crystalline Al₂O₃ at about 527 °C. The lower level of consolidation at 450 °C was mainly attributed to the fact that the native layer on the particle surfaces remained amorphous during HIP, and this rigid and coherent layer strongly limited the sintering of Al particles. However, the less tough crystalline alumina skeleton formed during sintering at 550 °C was broken due to the stresses developed during HIP, thereby creating Al/Al interfaces that facilitated the surface diffusion of Al atoms.

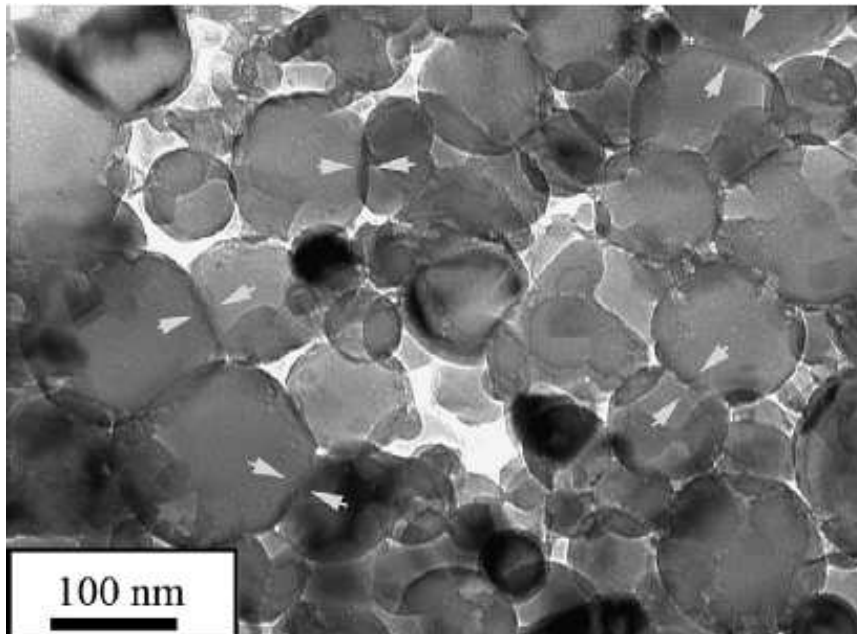


Fig. 4. TEM image of the Al sample consolidated at 450 °C. The white arrows indicate incipient sintering.

Summary

1. The SPS-processing of a Ni nanopowder in Ar resulted in a smaller grain-growth and therefore a higher strength due to the lower time and temperature of consolidation compared to the HIP procedure.
2. The smaller initial powder particle size yielded lower grain size and higher NiO content in UFG Ni consolidated by SPS. This resulted in higher strength but smaller strain to failure during compression as the oxide phase located at grain boundaries resulted in easier cracking during deformation. Similar tendencies were observed when the nanopowder was handled in air instead of Ar (even for limited time during die filling) before SPS-processing.
3. When sintering of an Al nanopowder was performed at 550 °C, the native amorphous layer on the surface of particles crystallized to alumina and fragmented into dispersoids that facilitated the diffusion of Al atoms during consolidation. However, during sintering at 450 °C the native layer remained amorphous and was not fragmented, hereby hindering the consolidation processes.

Acknowledgements

This work was supported in part by the Hungarian Scientific Research Fund, OTKA, Grant No. K-81360 and the French-Hungarian bilateral project (PHC Balaton, Hungarian Grant No. TeT_10-1-2011-0737). The European Union and the European Social Fund have provided financial support to this project under grant agreement no. TÁMOP 4.2.1./B-09/1/KMR-2010-0003. The authors are grateful for the financial of the French National Research Agency under the No. ANR-09-BLAN-0010-01 (MIMIC Project).

References

- [1] V. Viswanathan, T. Laha, K. Balani, A. Agarwal, S. Seal, Challenges and advances in nanocomposite processing techniques, *Mater. Sci. Eng. R* 54 (2006) 121–285.
- [2] H.V. Atkinson, S. Davies, Fundamental aspects of hot isostatic pressing: An overview, *Metall. Mater. Trans. A* 31 (2000) 2981–3000.
- [3] Q.H. Bui, G. Dirras, S. Ramtani, J. Gubicza, On the strengthening behavior of ultrafine-grained nickel processed from nanopowders, *Mater. Sci. Eng. A* 527 (2010) 3227–3235.
- [4] J. Gubicza, S. Nauyoks, L. Balogh, J. Lábár, T. W. Zerda, T. Ungár, Influence of sintering temperature and pressure on crystallite size and lattice defect structure in nanocrystalline SiC, *J. Mater. Res.* 22 (2007) 1314–1321.
- [5] J. Gubicza, H.-Q. Bui, F. Fellah, G. Dirras, Microstructure and mechanical behavior of ultrafine-grained Ni processed by different powder metallurgy methods, *J. Mater. Res.* 24 (2009) 217–226.
- [6] F. Tepper, Electro-explosion of wire produces nanosize metals, *Met. Powder Rep.* 53 (1998) 31–33.
- [7] Y. Kwon, Y. Jung, N. Yavorovsky, A. Illy, Ultra-fine powder by wire explosion method, *Scr. Mater.* 44 (2001) 2247–2251.
- [8] S. Billard, E. Meslin, G.F. Dirras, J.P. Fondère, B. Bacroix, Commercial purity aluminum with a bimodal grain size distribution: mechanical properties, deformation and fracture mechanisms, *J. Mater. Sci. Techn.* 20 (2004) 1–5.
- [9] B. Rufino, F. Boulch, M.V. Coulet, G. Lacroix, R. Denoyel, Influence of particles size on thermal properties of aluminium powder, *Acta Mater.* 55 (2007) 2815–2827.
- [10] S. Billard, J.P. Fondère, B. Bacroix, G.F. Dirras, Macroscopic and microscopic aspects of the deformation and fracture mechanisms of ultrafine-grained aluminum processed by hot isostatic pressing, *Acta Mater.* 54 (2006) 411–421.
- [11] G. Dirras, J. Gubicza, D. Tingaud, S. Billard, Microstructure of Al-Al₂O₃ nanocomposite formed by in-situ phase transformation during Al nanopowder consolidation, *Mater. Chem. Phys.* 129 (2011) 846–852.
- [12] P. Souza Santos, H. Souza Santos, S.P. Toledo, Standard transition aluminas. Electron microscopy studies, *Mater. Res.* 3 (2000) 104–114.